

## Pair Production by Electrons\*

M. CAMAC†

*Cornell University, Ithaca, New York*

(Received August 1, 1952)

Pair production by electrons was observed by measuring the positrons emitted from thin copper targets irradiated directly by the synchrotron electron beam ( $230 \pm 20$  Mev energy). The positrons were produced in either of two ways: either (1) directly by the electron beam, or (2) through a double process in which bremsstrahlung was first produced which then materialized in pairs in the same target. By measuring the positron rate as a function of target thickness a direct comparison of the two modes of production was obtained. The thickness of copper from which the positron yield was the same for both processes was  $0.0043 \pm 0.001$  inch ( $0.0073 \pm 0.0017$  radiation lengths). The positrons had about 0.80 of the energy of the incident electron beam.

The results of this experiment is shown to be in agreement with the Weizsaker-Williams approximation. In this approximation the formula for the number of virtual quanta associated with an incident electron contains a constant of the order of unity. Using the results of this experiment and the Bethe-Heitler formulas for the double process this constant was calculated to be  $1.6 \pm 0.2$ .

### I. INTRODUCTION

WITH the recent development of high energy electron accelerators detailed measurements of electromagnetic interactions are being extended to the several hundred million electron volt region. Measurements of the differential energy cross sections for bremsstrahlung<sup>1</sup> and pair production by gamma-radiation<sup>2</sup> were shown to be in agreement with the Bethe-Heitler formulas<sup>3</sup> modified slightly.<sup>4</sup> For the similar phenomenon of direct pair production by an electron, however, there were few quantitative measurements. In fact, this process was first observed<sup>5</sup> only recently in photographic plates irradiated in the upper atmosphere by cosmic radiation. With four events Hooper, King, and Morrish<sup>6</sup> obtained a rough measurement of the total cross section which was in agreement with the theoretical work of Racah and others.<sup>7</sup>

In the period from 1934 to 1941 there were several experimental attempts to measure direct pair production by electrons.<sup>8-12</sup> Except in two cases<sup>9,10</sup> cloud

chambers were used. In the more conclusive experiments<sup>11,12</sup> only upper limits to the cross section were obtained and these were not in disagreement with the theory. For example, Crane and Halpern<sup>12</sup> used a cloud chamber with  $\frac{1}{2}$ -mm lead plate in the center and an external source of beta-particles with energies ranging from 1 to 7 Mev. No events were observed in 1337 traversals of the plates. Recently there have been several abstracts on this phenomenon.<sup>13</sup>

The high energy electron accelerators furnish well-collimated, monochromatic electron beams and are ideally suited to measure pair production by electrons. Such measurements made with the Cornell synchrotron are described in this paper. The results are then compared to the theoretical work of Bhabha<sup>7</sup> and shown to be in agreement with the Weizsaker-Williams approximation.<sup>14</sup>

### II. EXPERIMENTAL APPARATUS

A schematic section in the median plane of the synchrotron indicating the detecting apparatus and the modifications in the donut-shaped vacuum system is shown in Fig. 1.

The well-collimated<sup>15</sup> electron beam expanded outward from its accelerating orbit and irradiated a thin copper target. The expanded beam was used in order to minimize the time that the outgoing positrons spent in the strong magnetic field, which decreased their energy dispersion. The predominant radiation produced in the target (electrons, positrons and bremsstrahlung) initially travelled in the direction of the incident beam. The components were then separated by the strong magnetic field: the electrons circled inward; the gamma radiation went tangent to the orbit; and the positrons

\* This research supported jointly by the ONR and AEC.

† Now at the University of Rochester, Rochester, New York.

<sup>1</sup> J. W. DeWire and L. A. Beach, *Phys. Rev.* **83**, 476 (1951).

<sup>2</sup> G. D. Adams, *Phys. Rev.* **74**, 1707 (1948); R. L. Walker, *Phys. Rev.* **76**, 527 (1949); J. L. Lawson, *Phys. Rev.* **75**, 433 (1949); Powell, Hartsough, and Hill, *Phys. Rev.* **81**, 213 (1951); DeWire, Beach, and Ashkin, *Phys. Rev.* **83**, 233, 476, 505 (1951); **82**, 447 (1951).

<sup>3</sup> W. Heitler, *The Quantum Theory of Radiation* (Oxford University Press, London, 1944).

<sup>4</sup> L. C. Maximon and H. A. Bethe, *Phys. Rev.* **87**, 156 (1952); Handel Davies and H. A. Bethe, *Phys. Rev.* **87**, 156 (1952).

<sup>5</sup> Bradt, Kaplon, and Peters, *Helv. Phys. Acta* **23**, 43 (1950); **24**, 23 (1950); G. P. S. Occhialini, *Nuovo cimento Supp.* **6**, 3, 413 (1949).

<sup>6</sup> Hooper, King, and Morrish, *Phil. Mag.* **42**, 304 (1951).

<sup>7</sup> G. Racah, *Nuovo cimento* **14**, No. 3, 93 (1937); H. J. Bhabha, *Proc. Roy. Soc. (London)* **152**, 559 (1935); D. G. Ravenhall, *Proc. Phys. Soc. (London)* **113**, 1177 (1950); (private communication).

<sup>8</sup> Sizoo, Barendregt, and Griffioen, *Physica* **7**, 860 (1940).

<sup>9</sup> J. R. Feldmeier and G. B. Collins, *Phys. Rev.* **58**, 200 (1940).

<sup>10</sup> N. Feather and J. V. Dunworth, *Proc. Cambridge Phil. Soc.* **34**, 435 (1938).

<sup>11</sup> Hans Staub, *Helv. Phys. Acta* **9**, 306 (1939).

<sup>12</sup> H. R. Crane and J. Halpern, *Phys. Rev.* **55**, 838 (1939).

<sup>13</sup> Cleland, Konneker, and Hughes, *Phys. Rev.* **79**, 229 (1950); M. Camac, *Phys. Rev.* **83**, 207 (1951); N. J. Shiren and R. F. Post, *Phys. Rev.* **86**, 617 (1952).

<sup>14</sup> C. F. v. Weizsaker, *Z. Physik* **88**, 612 (1934); E. J. K. Williams, *Kgl. Dansk Videnskab. Selskab, Mat.-fys. Medd.* **13**, 4 (1935); *Phys. Rev.* **45**, 729 (1934).

<sup>15</sup> In the region of the target the beam was approximately 2 mm high and 4 mm wide.

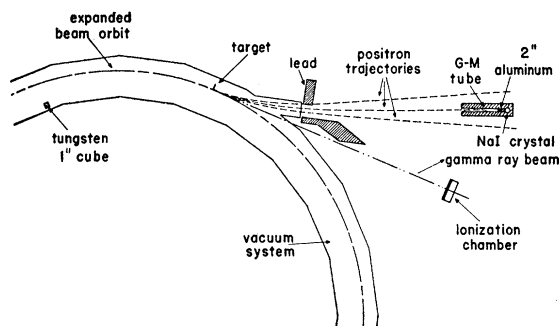


FIG. 1. Experimental arrangement indicating the modifications in the vacuum system of the synchrotron, shielding and the radiation detectors.

spiraled outward and were separated in energy. Trajectories for three different energies are shown in Fig. 1. The path with the least curvature is for a positron with the same energy as the primary electron. The next is for 0.8 of the initial energy and the most curved one is for 0.6. The position of the target was chosen so that the high energy positrons left the vacuum system through a thin  $\frac{1}{32}$ -inch aluminum exit port.

The target and target holder used in the final runs are shown in Fig. 2. The targets were copper strips  $\frac{1}{4}$  inch in the vertical direction, 0.050 inch in the radial direction, and a range of thicknesses in the azimuthal direction, 0.0012, 0.0040, 0.0104, and 0.0160 inch. The copper targets were cemented to polystyrene strips 0.020 inch by 0.010 inch which were mounted on 0.040-inch "C" shaped Lucite rings. A coating of Aquadag was placed on all plastic parts to avoid electrical charging. There were provisions (1) for rotating this target assembly out of the beam and (2) moving it azimuthally in the donut.

The positron detector was a lead shielded counter telescope consisting of a thin walled G-M tube, 2 inches of aluminum, and a 4-cm by 4-cm NaI scintillation detector set to record signals greater than about 15-Mev energy. A charged particle at minimum ionization must have had at least 40-Mev energy to produce a coincidence pulse in the two detectors. The coincidence system served two purposes: (1) It set an energy bias on the particles to be measured, and (2) it discriminated against gamma-radiation. The positron detector was mounted on a bakelite table between the synchrotron magnet coils and the back column of a magnet yoke. Two selsyn drives remotely controlled (1) the rotation and (2) the azimuthal translation of the telescope.

The bremsstrahlung beam from the target was measured with an ionization chamber with  $\frac{1}{4}$  inch of lead in front of it.

The electronic circuits were of standard design. The positron detector was sensitive to radiation only during the target irradiation time.

Radiation shielding was placed around the exit port and inside the donut (see Fig. 1). The lead at the port shielded against gammas and low energy positrons from

the target. The tungsten cube prevented the degraded electrons from striking the portion of the inner wall of the donut from which gamma-rays would go in the direction of the positron detector.

### III. IDENTIFICATION OF THE POSITRONS

The identification of the positrons was obtained with two complementary measurements. It was ascertained (1) that the particles had the curvature in the magnetic field and intensity distribution that was theoretically predicted for positrons, and (2) that they came from the target. For thick targets a calculated distribution was possible since the pairs were produced mainly through the double process with the intermediate bremsstrahlung beam.

The measurements were made as follows. A 0.040-inch tungsten wire was used for the target. The azimuthal positions of the target and positron telescope detector were fixed. The counting rate in the positron counters was measured as a function of the telescope rotation for a constant integrated bremsstrahlung beam. Typical data are shown in Fig. 3. The abscissa is plotted in degrees of rotation with  $0^\circ$  for the telescope pointing to the center of the synchrotron. At the setting of the

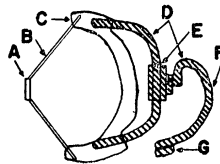


FIG. 2. Target and target holder. A: copper target; B: 0.010-inch polystyrene strips; C: 0.040-inch Lucite; D: stainless steel; E: target rotated in and out of beam on this axis; F: this point rested against wall of vacuum system; and G: shaft to exit port plate to support target assembly.

peak, about  $30^\circ$ , the telescope pointed towards the exit port.

Next, the counter telescope was moved azimuthally to observe positrons of different energies. For each translational position the telescope was rotated to determine the rate at the peak of the curve. In Fig. 4 the counting rates at the peak of the curves are plotted as a function of the azimuthal position of the counter telescope. Each point is normalized to the same integrated gamma-ray beam. Also shown in Fig. 4 is the theoretically expected distribution for thick targets, such as the 0.040-inch tungsten wire. The agreement is very good. This distribution was obtained by folding the Bethe-Heitler differential energy formulas for the double process with the energy dispersion curves for the synchrotron magnetic field. The degree markers plotted along the abscissa represent the angle between the positron detector and the target with the vertex at the center of the synchrotron.  $37.75^\circ$  was the detector position for positrons with the same energy as the synchrotron beam.

Experimental data represented in Fig. 4 were repeated for different azimuthal positions of the target. The angular shift of the curve as shown in Fig. 4 corresponded to the angular motion of the target. Thus, the

37.75° end point remained the same. From the above measurements we concluded that we were observing positrons.

#### IV. THEORY OF THE MEASUREMENTS

There are only two important ways in which positrons can be created in the target by the electron beam: (1) by direct pair production by electrons and (2) by the double process in which the bremsstrahlung gamma-rays produce pairs in the same target. The yield from the direct process varies linearly with target thickness. For the double process the variation is quadratic. Thus, by measuring the positron rates for different target thicknesses the two processes were separated. This simple theory was applied to the measurements as follows.

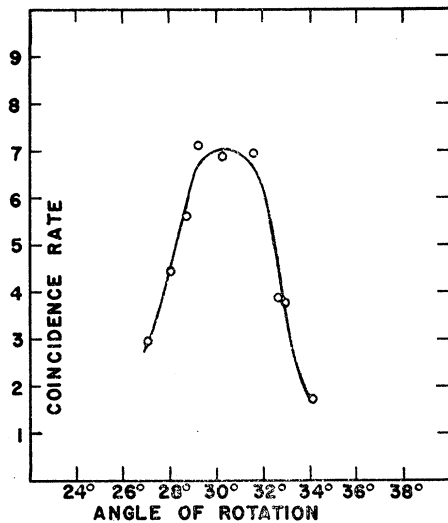


FIG. 3. Coincidence counting rate as a function of angle of rotation of positron detector for fixed positions of the target and detector. All points normalized in the same integrated bremsstrahlung beam. At the rotation angle of 0° the detector pointed to the center of the synchrotron.

Let  $P$  be the total positron count arising from both processes.

$$P = (\text{direct process}) + (\text{double process}). \quad (1)$$

$$P = (e_s t B) + (\frac{1}{2} e_d D^2 B), \quad (2)$$

where  $e_s$  and  $e_d$  are the detection efficiencies for the direct and double process;  $S$  and  $D$  are the cross sections per radiation length of target for producing positrons by the direct and double process, respectively;  $t$  is the target thickness and  $B$  is the integrated incident beam. The factor of  $\frac{1}{2}$  in the term for the double process arises since the same target is used for the two interactions. Since all the positrons leave the target in the same direction, we cannot determine directly from which process they were produced. Thus, they will be detected with equal efficiency, i.e.,  $e_s = e_d$ . The formula

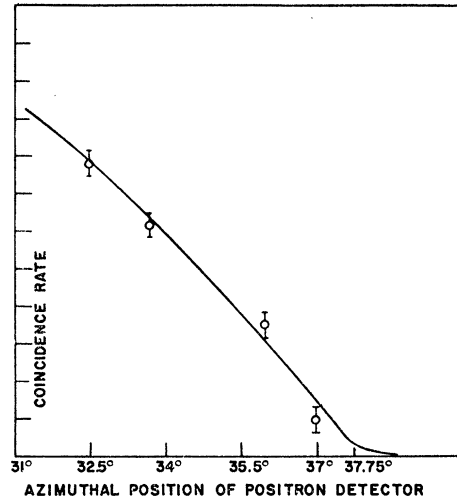


FIG. 4. Experimental points indicate the coincidence rates at the peaks of the detector rotation curves for different azimuthal positions of the positron detector. The angle notation on the abscissa axis is the angle between the target and the detector with the vertex at the center of the synchrotron. The curve is the theoretical distribution of the positrons.

for  $P$  becomes

$$P = e_s t B (S + \frac{1}{2} D t). \quad (3)$$

The total gamma-ray counts, say  $G$ , was

$$G = g t B, \quad (4)$$

where  $g$  is the total gamma-ray counts per radiation length of target;  $t$  and  $B$  are the same as in Eq. (2).

In this experiment the ratio  $P/G$  was measured:

$$P/G = e_s t B (S + \frac{1}{2} D t) / B g t. \quad (5)$$

$$P/G = (e_s/g) (S + \frac{1}{2} D t). \quad (6)$$

Note that the expression for  $P/G$  varies linearly with target thickness. The parenthesis in Eq. (6) does not contain terms that depend upon the detection efficiency. This enormously simplified the experiment. The final results are independent of the efficiencies of the positron and gamma ray detectors.

If we extrapolate the linear curve of Eq. (6) to the point where  $P/G = 0$ , then the value of the parenthesis is zero. Let  $t = t_0$  at this extrapolated point. We obtain the relation for the cross section for direct pair production:

$$S = -\frac{1}{2} D t_0. \quad (7)$$

A physical interpretation can be given to  $t_0$ . The probability for an electron to create a positron of a definite energy in passing through a target thickness  $t_0$  is the same for the direct and double process.

The cross sections for the double process have been experimentally determined<sup>1,2</sup> and are given by the Bethe-Heitler formulas<sup>3</sup> modified slightly.<sup>4</sup> The value of  $t_0$  was obtained in this experiment. Thus, the absolute value of the pair production by electrons differential

TABLE I. Measurements of pair production.

Ratio of positron to incident electron energy	Thickness of copper target (inches)	Uncorrected data including standard error	Corrected data
0.83	0.0012	390±15	390±15
	0.0040	510±15	510±15
	0.0104	1050±15	1060 <sup>+55</sup> <sub>-15</sub>
	0.0160	1320±20	1420 <sup>+130</sup> <sub>-100</sub>
0.78	0.0012	455±10	455±10
	0.0040	675±20	675±20
	0.0104	1170±20	1181 <sup>+60</sup> <sub>-20</sub>
	0.0160	1750±20	1890 <sup>+180</sup> <sub>-140</sub>

cross section can be obtained by combining the results of this experiment with the formulas for the double process.

### V. MEASUREMENTS

In the analysis of this experiment it is convenient to express the energy of the positron in two steps:

- (1) the energy of a positron relative to that of its incident beam electron, and
- (2) the energy of the incident electron.

The trajectories of the positions depended only on the relative energy and were independent of the energy of the electron beam.

The synchrotron beam irradiated the target for one millisecond starting at the time that the expanded beam conditions set in. Although about 315 Mev was available with the contracted beam, the expanded beam was limited to 250-Mev energy. Since the magnetic field was decreasing during the irradiation time, the beam energy dropped proportionately to about 210 Mev. Thus, the energy of the electron beam was 230±20 Mev. These values were obtained by comparing the magnitude of the magnetic field at the top of the magnetic cycle to that at the time of the target irradiation. At the top of the cycle the magnetic field was measured in two ways: (1) directly and (2) by an analysis of the data on the bremsstrahlung spectrum.

The ratio of a positron's energy to its incident beam electron was not obtained directly by measurements, but from the calculation of the positron spectral yield as a function of the positron telescope position as shown in Fig. 3. The uncertainty in the energy determination by this method was about 5 percent.

Consistent data was obtained with the positron detector at two azimuthal positions corresponding to energies of about 0.83 and 0.78 of the energy of the incident electron beam. It was difficult to obtain data with positrons of other energies. For a ratio of energies significantly greater than 0.83 insufficient shielding from the gamma-radiation from the target and the small counting rates were the limiting factors. For energies lower than 0.78, the positron trajectories were

either too curved to leave the small two-inch exit port of the vacuum system or they met obstacles in the region of the magnet coils.

The results of the measurements of the cross section for pair production are shown in Table I. Four copper foils of different thicknesses were used for targets: 0.0012, 0.0040, 0.0104, and 0.0160 inch.

The positron count *versus* telescope rotation was taken for each azimuthal setting and each target thickness, and the intensity at the peak of the curve was determined within a few percent statistics. The values at the peak together with their standard error are shown in Table I under the column heading "Uncorrected data." These were normalized to a constant integrated bremsstrahlung beam.

Corrections to this data for (1) background, (2) multiple scattering of the incident beam and positrons in the target, (3) target misalignment, and (4) other sources will be discussed in the next section. The results including these corrections are tabulated in the last column of Table I.

These corrected positron counts are plotted in Fig. 5 as a function of target thickness. According to the discussion in Sec. IV, straight lines should be drawn between readings taken at a fixed translational setting.

For the limits of uncertainty of the extrapolated thickness  $t_0$  determined from the data shown in Fig. 5, the final results are

$$|t_0| = 0.0046 \pm 0.0008 \text{ inch for the ratio of positron to incident electron energy of 0.78;}$$

$$|t_0| = 0.0043 \pm 0.0010 \text{ inch for the ratio of positron to incident electron energy of 0.83.}$$

### VI. CORRECTIONS TO THE MEASUREMENTS

In this section the following corrections to the measurements will be discussed: (1) background, (2) multiple scattering in the target, (3) target misalignment with respect to synchrotron beam, and (4) other corrections. These corrections were included in the last column of Table I.

(1) Background: All background was produced by gamma-radiation either from the target or from electrons striking other parts of the donut. By removing the target from the beam it was found that less than 3 percent of the counts were produced by radiation from other parts of the donut. By an analysis of the data taken with lead and without lead at the exit port it was found that the number of gamma-ray counts was not larger than the statistical error of about 5 percent. The main background radiation varied linearly with the thickness of the target and, thus, increased the measured value of the direct positron production. Thus, the values for  $t_0$  determined in Sec. V are upper limits.

(2) Multiple scattering in the target: Multiple scattering in the target of the incident electrons and outgoing positrons spread the positron trajectories at

the detector. Multiple scattering in the median plane of the synchrotron did not produce a change in the counting rate because of the contribution of positrons of neighboring energies. However, this produced a spread in the energy of the positrons entering the detector. Multiple scattering in the vertical direction (normal to the median plane) did produce a loss of positrons for thick targets. The loss was determined by varying the vertical aperture of the detector. There were no losses for the 0.0012- and 0.0040-inch targets, about 1 percent loss for the 0.0104-inch target, and  $8 \pm 6$  percent loss for the 0.0160-inch target.

(3) Misalignment of target: When this experiment was started it was felt that one of the major limitations would be the determination of the thickness of the target. The radial expansion of the beam was so slow compared to the time for an orbit revolution that on the average one would expect a radial penetration of about 0.0001 to 0.0002 inch. One could not hope to prepare thin foils with edges that were uniform in regions of this size and then to line up the foils perpendicular to the beam to fractions of a degree.

A systematic set of measurements (to be published elsewhere) were made to determine the irradiation pattern of the foil, and they showed that the picture of the previous paragraph was incorrect. On the contrary, not only did the beam radially penetrate well into the foil, but especially for the thin targets a large region of the donut, up to an inch in diameter, was irradiated. In fact, minimization of the radiation from the target supports became an important problem.

In the primary traversal of the target the vertical extension of the beam was roughly two millimeters. In the primary traversal of the target the beam irradiation decreased almost exponentially with radial penetration—a drop by a factor 2 in from 0.002 to 0.003 inch becoming negligible at about 0.015 inch. During the first traversal the beam was multiply scattered and spread out. It was then able to irradiate a greater region of the target and even the target holder in the subsequent traversals. The subsequent traversals in the 0.0012, 0.0040, 0.0104, and 0.0160 inch foils were 9, 3.2, 0.6, and 0.3, respectively. Thus, we see that for the thin foils the primary traversal was a small part of the total irradiation.

From the above measurements it was shown that the effects of the target supports were most important for the thinnest target. With the design used the target supports produced a 1 percent effect for the 0.0012-inch target and was negligible for the others.

Misalignment of the target with respect to the synchrotron beam did not change the direct positron production but decreased the yield from the double effect for a constant integrated bremsstrahlung beam. The effect was more important for the thick targets. Unfortunately the target was not aligned directly with the synchrotron beam, but on a model of the synchrotron donut. While the alignment with the model was

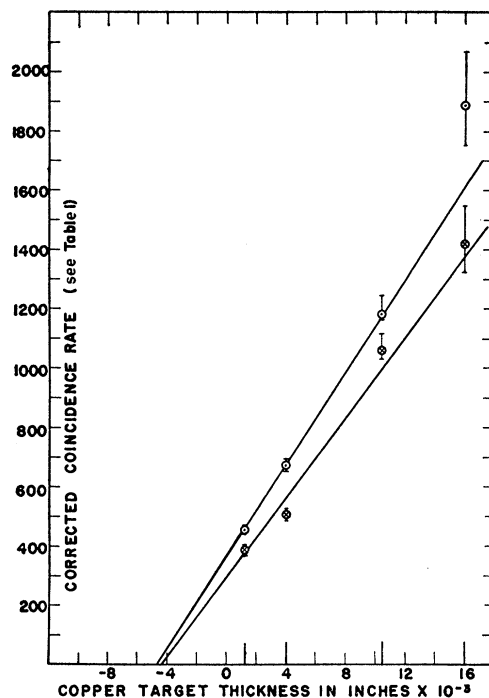


Fig. 5. Corrected positron counting rate as a function of the target thickness. Data taken from the last column of Table I. Upper curve: data for positrons with 0.78 of the energy of the incident beam. Lower curve: data for positrons with 0.83 of the energy of the incident electron beam.

better than  $3^\circ$  an over-all misalignment uncertainty of about  $5^\circ$  was used. This introduced uncertainties of 0 percent, 1 percent, 4 percent, and 9 percent for the 0.0012, 0.0040, 0.0104, and 0.0160 inch targets, respectively.

(4) Other sources of errors were considered, such as electronics stability, beam fluctuations, etc., but no corrections were needed for them.

## VII. CONCLUSIONS

The results of this experiment were compared to the theoretical work of Bhabha.<sup>7</sup> He showed that within the accuracy of his calculations the Weizsaker-Williams approximation gave the same result as the usual quantum mechanical treatment.

In this approximation one essentially compares the virtual quanta spectrum associated with the incident electron for producing the direct pair production to the bremsstrahlung gamma-rays for the double process. It is assumed that the cross section for pair production is the same for the virtual and real gamma-rays.

The virtual gamma-ray spectrum is given by the formula:

$$N(\gamma)d\gamma = \frac{2\pi}{137} \frac{d\gamma}{\gamma} \log\left(\frac{k}{\gamma}\right), \quad (8)$$

where  $N$  is the number of quanta with energy between  $\gamma$  and  $\gamma+d\gamma$ ;  $\gamma$  is the ratio of the quanta to the incident

electron energy; and  $k$  is a constant of the order of unity.

With this approximation the formula for the extrapolated thickness  $t_0$  [see Eq. (7)] becomes

$$|t_0| = \frac{2S}{D} = \frac{2 \int_n^1 N(\gamma) \frac{d\gamma}{\gamma} \phi\left(\gamma, \frac{n}{\gamma}\right)}{\int_n^1 \Psi(E_s, \gamma) \frac{d\gamma}{\gamma} \phi\left(\gamma, \frac{n}{\gamma}\right)}, \quad (9)$$

where  $n$  is the ratio of the positron energy to the incident electron energy,  $E_s$ ;  $\Psi$  and  $\phi$  are the Bethe-

Heitler formulas<sup>3,4</sup> for bremsstrahlung and pair production, respectively; and  $N$  and  $\gamma$  are the same as in Eq. (8). Substituting the result of this experiment for  $t_0$  the arbitrary constant  $k$  in the formula for the virtual quanta spectrum was calculated:

$$k = 1.6 \pm 0.2. \quad (10)$$

This is in agreement with the Weizsaker-Williams approximation.

I wish to thank Professor R. R. Wilson for his continuous interest and guidance. The author is also indebted to Professor D. R. Corson for measuring the beam energy for this experiment.

## Symmetrical Pseudoscalar Meson Theory of Nuclear Forces\*

JOSEPH V. LEPORE

Radiation Laboratory, Department of Physics, University of California, Berkeley, California

(Received July 25, 1952)

Nuclear forces yielded by the symmetrical pseudoscalar theory are discussed in terms of a perturbation expansion. It is shown that, up to terms in the square of the coupling constant, the pseudoscalar coupling is equivalent to a scalar pair coupling of the pseudoscalar field plus a pseudovector coupling of that field. The dominant contribution to the fourth-order nucleon potential is then obtained in a simple way by using this result.

### INTRODUCTION

THE nuclear force given by the symmetrical pseudoscalar meson theory with pseudoscalar coupling has been re-examined in recent years by a number of authors<sup>1</sup> treating the meson-nucleon interaction as weak. They have shown that the contribution to these forces due to processes involving transport of momentum between nucleons by a pair of mesons are larger than those due to a single meson. The pseudoscalar character of the meson implies that simultaneous emission or absorption of  $S$ -state meson pairs by a single nucleon cannot involve nucleon spin change. Similarly the symmetrical theory implies that there can be no isotopic spin change for these processes. As a consequence the forces due to them are spin and charge independent.

The importance of these effects suggests that one should be able to exhibit them explicitly in the meson-nucleon interaction Hamiltonian. In what follows the nuclear forces are obtained in a simple manner by taking advantage of this possibility. Besides having the aforementioned properties it is shown that these forces are highly singular and have a range of half the meson Compton wavelength.

\* This work was performed under the auspices of the AEC.

<sup>1</sup> K. M. Watson and J. V. Lepore, Phys. Rev. **76**, 193 (1949) and Phys. Rev. **76**, 1157 (1949); H. A. Bethe, Phys. Rev. **76**, 191 (1949); Y. Nambu, Prog. Theoret. Phys. **5**, 4, 614 (1950); R. P. Feynman, California Institute of Technology lecture notes (unpublished).

### I. TRANSFORMATION OF THE HAMILTONIAN

The equation of motion, in the interaction representation,<sup>2</sup> of the state vector,  $\Psi[\sigma]$ , of the coupled meson and nucleon fields is determined by the coupling Hamiltonian

$$H(x) = i f \bar{\psi}(x) \gamma_5 \tau_\alpha \psi(x) \phi_\alpha(x). \quad (1)$$

Here and in the following  $\psi$ ,  $\bar{\psi}$ ,  $\phi$  represent the nucleon and meson field variables,  $\tau_\alpha$  is the nucleon isotopic spin and  $\gamma_5 = \gamma_1 \gamma_2 \gamma_3 \gamma_4$  is the Dirac pseudoscalar. Units are chosen so  $\hbar = c = 1$  and the meson and nucleon masses are  $\mu$  and  $K_0$ , respectively.

If one now applies the transformation  $e^{iS[\sigma]}$  used by Dyson,<sup>3</sup>

$$S[\sigma] = - \frac{if}{2K_0} \int d\sigma_\mu \bar{\psi}(x) \gamma_\mu \gamma_5 \tau_\alpha \phi_\alpha(x) \psi(x), \quad (2)$$

to the state vector  $\Psi[\sigma]$ ,

$$\Psi[\sigma] = e^{iS[\sigma]} \Psi'[\sigma], \quad (3)$$

one finds that the new Hamiltonian is, up to terms in  $f^3$ ,

$$H'(x) = H(x) - i[S[\sigma], H(x)]$$

$$+ \frac{\delta S[\sigma]}{\delta \sigma(x)} - \frac{i}{2} \left[ S[\sigma], \frac{\delta S[\sigma]}{\delta \sigma(x)} \right]. \quad (4)$$

<sup>2</sup> J. S. Schwinger, Phys. Rev. **74**, 1439 (1948).

<sup>3</sup> F. J. Dyson, Phys. Rev. **73**, 929 (1948).